Provided for non-commercial research and education use.
Not for reproduction, distribution or commercial use.

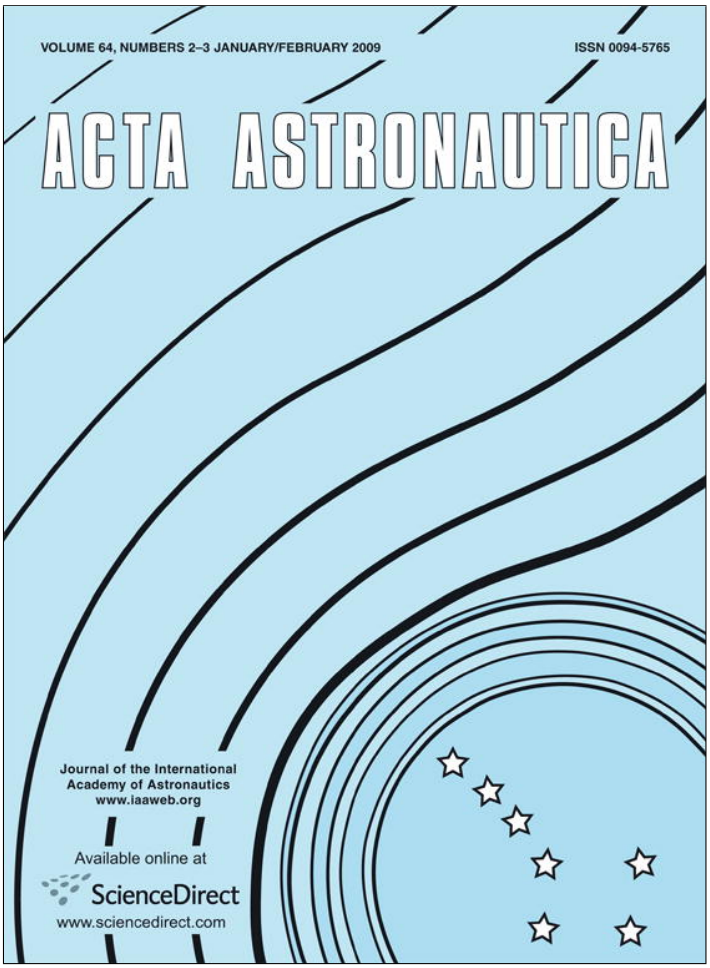

This article appeared in a journal published by Elsevier. The attached copy is furnished to the author for internal non-commercial research and education use, including for instruction at the authors institution and sharing with colleagues.

Other uses, including reproduction and distribution, or selling or licensing copies, or posting to personal, institutional or third party websites are prohibited.

In most cases authors are permitted to post their version of the article (e.g. in Word or Tex form) to their personal website or institutional repository. Authors requiring further information regarding Elsevier's archiving and manuscript policies are encouraged to visit:

http://www.elsevier.com/copyright

Author's personal copy

PERGAMON

Available online at www.sciencedirect.com
ScienceDirect

Acta Astronautica 64 (2009) 188–194

ACTA ASTRONAUTICA

www.elsevier.com/locate/actaastro

Subcooled pool boiling on thin wire in microgravity

J.F. Zhao*, S.X. Wan, G. Liu, N. Yan, W.R. Hu

National Microgravity Laboratory/CAS, Institute of Mechanics, Chinese Academy of Sciences, 15 Beisihuan Xilu, Beijing 100190, China

Received 22 December 2006; received in revised form 18 June 2008; accepted 3 July 2008
Available online 8 August 2008

Abstract

A new set of experimental data of subcooled pool boiling on a thin wire in microgravity aboard the 22nd Chinese recoverable satellite is reported in the present paper. The temperature-controlled heating method is used. The results of the experiments in normal gravity before and after the flight experiment are also presented, and compared with those in microgravity. The working fluid is degassed R113 at 0.1 MPa and subcooled by 26 °C nominally. A thin platinum wire of 60 μm in diameter and 30 mm in length is simultaneously used as heater and thermometer. It is found that the heat transfer of nucleate pool boiling is slightly enhanced in microgravity comparing with those in normal gravity. It is also found that the correlation of Lienhard and Dhir can predict the CHF with good agreement, although the range of the dimensionless radius is extended by three or more decades above the originally set limit. Three critical bubble diameters are observed in microgravity, which divide the observed vapor bubbles into four regimes with different sizes. Considering the Marangoni effect, a qualitative model is proposed to reveal the mechanism underlying the bubble departure processes, and a quantitative agreement can also be acquired.
© 2008 Elsevier Ltd. All rights reserved.

Keywords: Nucleate pool boiling; Microgravity; Subcooling; Bubble departure diameter

1. Introduction

Pool boiling in microgravity has become an increasing significant subject for investigation, since many potential applications exist in space and on planetary neighbors due to its high efficiency. However, the investigation in microgravity suffers for unique and stringent constraints in terms of size, power and weight of experimental apparatuses, and of number and duration of the experiments. Thus, only a partial and in some aspects contradictory knowledge of microgravity boiling has been attained so far. On the progress in this field, several comprehensive reviews, such as Straub [1] and Di Marco and Grassi [2] among many others, are available.

Boiling is a very complex and illusive process because of the interrelation of numerous factors and effects as the nucleate process, the growth of the bubbles, the interaction between the heater's surface with liquid and vapor, the evaporation process at the liquid–vapor interface, and the transport process of vapor and hot liquid away from the heater's surface. For a variety of reasons, fewer studies have focused on the physics of the boiling process than have been tailored to fit the needs of engineering endeavors. As a result, the literature has been flooded with the correlations involving several adjustable, empirical parameters. These correlations can provide quick input to design, performance, and safety issues and hence are attractive on a short-term basis. However, the usefulness of the correlations diminishes

* Corresponding author. Tel.: +86 10 82544129; fax: +86 10 82544096.
E-mail address: jfzhao@imech.ac.cn (J.F. Zhao).

0094-5765/$ - see front matter © 2008 Elsevier Ltd. All rights reserved.
doi:10.1016/j.actaastro.2008.07.004

Author's personal copy

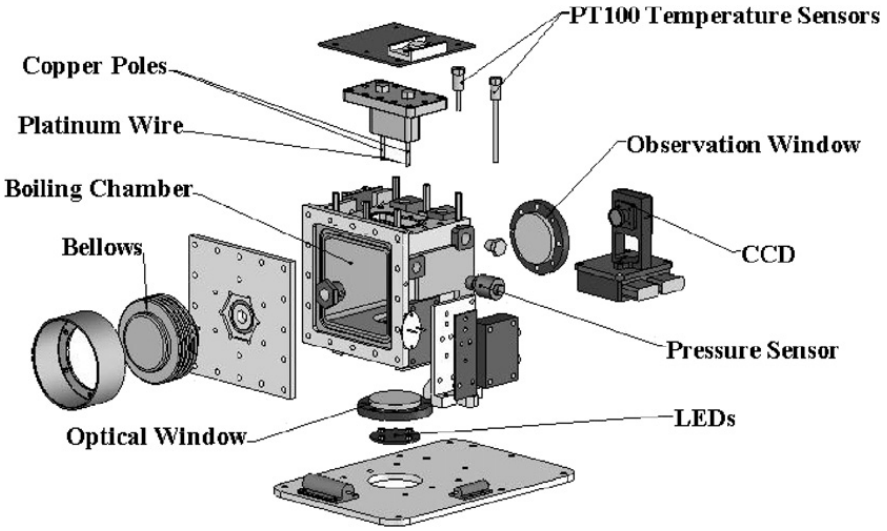

Fig. 1. Diagram of boiling chamber and its accessories.

very quickly as parameters of interest start to fall outside the range of physical parameters for which the correlations were developed. Thus, the physics of the boiling process itself is not properly understood yet, and is poorly represented in the most correlations, despite almost seven decades of boiling research.

The present work is a research effort on subcooled pool boiling heat transfer both in normal gravity on Earth and in microgravity aboard the 22nd Chinese recoverable satellite. The results of the experiments, particularly those in the nucleate boiling region, are presented and analyzed here.

2. Experimental facility

A temperature-controlled pool boiling (TCPB) device (Fig. 1) has been developed to perform such studies. Detailed description of the experimental facility can be read in Wan et al. [3].

A platinum wire of 60 μm in diameter and 30 mm in length is simultaneously used as the heater and thermometer, with the advantage that it is very sensible to changes in temperature and heat flux because of its low thermal capacity. The ends of the wire are soldered with copper poles of 3 mm in diameter to provide a firm support for the wire heater and low resistance paths for the electric current. The heater resistance, and thus the heater temperature, is kept constant by a feedback circuit similar to that used in constant-temperature hot-wire anemometry.

The working fluid is degassed R113 with nominally a volume of 700 ml. Two platinum resistance thermometers with a range of 0–60 °C are used to measure the bulk temperature of the fluid in the boiling chamber, which are calibrated to within 0.25 °C. The absolute pressure within the boiling chamber is measured using a pressure transducer with a range of 0–0.2 MPa and an accuracy of 0.25%FS (full scale). Two LEDs (light-emitting diode) are used to light the boiling chamber through a window at the chamber bottom. A CCD video camera is used to obtain images of vapor bubbles or film around the heater, which is recorded at a speed of 25 FPS (frame per second).

The voltages across the heater and a reference resistance, which is used to measure the electric current through the heater, are sampled at 20 Hz. The outputs of the pressure transducer and the platinum resistance thermometers are sampled at $\frac{1}{3}$ Hz. A sample rate of 1000 Hz for every data channel is used in ground experiments. The analysis shows that using the higher sample rate can significantly reduce the uncertainty of the heater temperature, while negligible influence is found on the uncertainty of heat flux. Thus, in the following data reduction, temperatures for 16 set-points are determined based on the data obtained from the higher sample rate on the ground, while heat fluxes are determined based on measured data in experiments. The uncertainty of the heater temperature is less than 3 °C, and that of the heat flux is less than 24 kW/m^2 in space experiment and 21 kW/m^2 in ground experiments, respectively.

3. Experimental results

3.1. Comparison between heat flux in normal and microgravity

Detailed conditions of the space and ground experiments are listed in Table 1. The pressure and the

Author's personal copy

Table 1
Experimental conditions of space and ground experiments.

	Pressure(kPa)	T_l(°C)	ΔT_{sub}(°C)
Ground experiment before the flight	101.2	22.1	25.5
Space experiment	101.0	21.3	26.2
Ground experiment after the flight	101.4	20.5	27.1

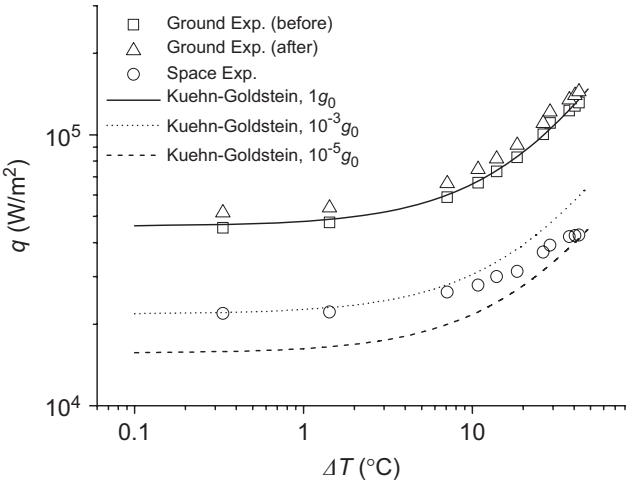

Fig. 2. Single phase convection.

subcooling of the bulk liquid are normally 0.1 MPa and 26 °C, respectively.

The first heat transfer mode is single-phase natural convection both in normal gravity and in microgravity. The comparison between data and the common used relation of Kuehn and Goldstein [4] is shown in Fig. 2. For the ground experiments, an agreement is quite evident, which warrants reasonable confidence in the data. Comparison between the results of space experiments and the predictions indicates that the residual gravity during the space experiment is between 10^{-3} and 10^{-5} g_0, which is equivalent to that given by the satellite establishment.

The onset of boiling occurs at the 16th set-point as two-mode transition boiling both in the space experiment and in ground experiments. The temperature at the onset of boiling is 83.2 °C, which is independent, or at least, dependent much weakly on gravity. Detailed analysis on the data of two-mode transition boiling will be presented elsewhere in the future.

Fig. 3 shows the variety of heat flux near the critical heat flux (CHF) in different gravity levels. Steady nucleate boiling is observed with high heat flux in the 42nd set-point of the heater temperature ($T_{W,42}$). When

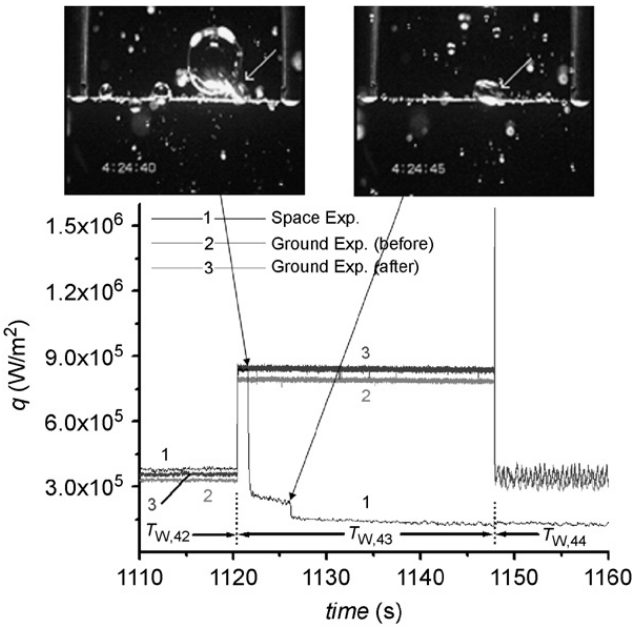

Fig. 3. Heat flux near the CHF in different gravity.

the set-point of the heater temperature changed upward from $T_{W,42}$ to $T_{W,43}$ in the space experiments, the heat flux is ascending to another steady nucleate boiling state with a higher heat flux. This state, however, cannot be kept after about 1 s. A quick drop is observed which is caused by the appearance of two-mode transition boiling. From the video record, it is found that a middle bubble on the right side of the heater was coalesced by a large departed bubble, the vibration due to the coalescence of bubbles leads to the fact that a vapor film covers the heater on the location of the middle bubble. Therefore, the CHF should locate between $T_{W,42}$ and $T_{W,43}$, giving the range of CHF in microgravity as $(3.8–8.4) \times 10^5\,W/m^2$. In ground experiments, a new steady nucleate boiling state can be maintained for the whole duration of about 30 s when the set-point of the heater temperature changed upward from $T_{W,42}$ to $T_{W,43}$. Two-mode transition boiling occurs when the set-point of the heater temperature changed upward from $T_{W,43}$ to $T_{W,44}$. Thus, the CHF, or more accurately, the lower limit of CHF, can be determined as 7.9×10^5 and $8.4 \times 10^5\,W/m^2$ for the ground experiments before and after flight, respectively.

Fig. 4 plots the results of nucleate boiling obtained in the space and ground experiments. In both the space experiment and ground experiments, the boiling curve of up-stepping process is lower than that of down-stepping process due to the difference of bubble behaviors on the heater surface. It is also shown that except one point of $\Delta T_{sat} = 7.4$ °C during the 2nd up-stepping of

Author's personal copy

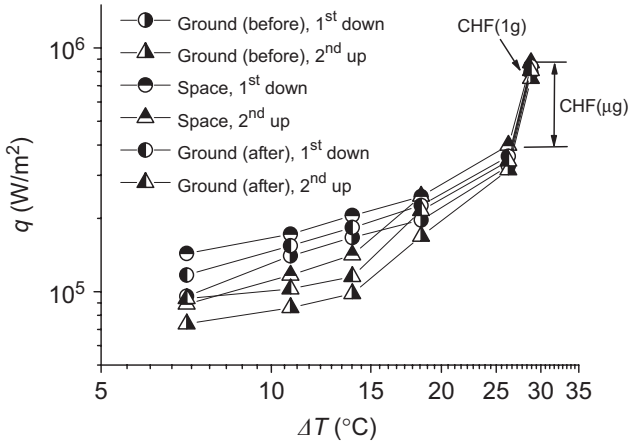

Fig. 4. Nucleate boiling curves in different gravity.

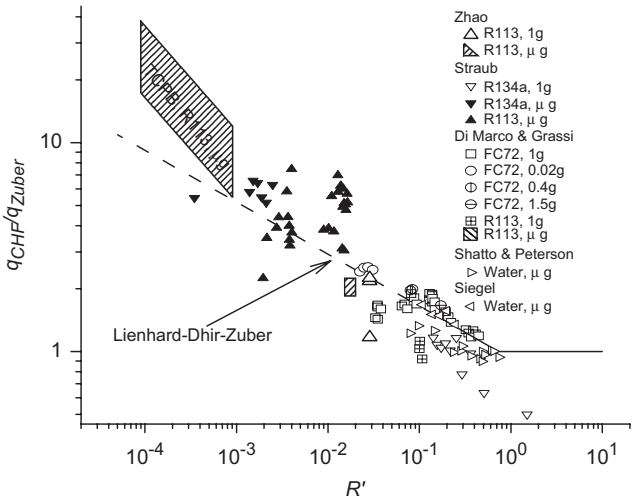

Fig. 5. Scaling of CHF with gravity.

temperature, the heat transfer of nucleate pool boiling in microgravity is slightly enhanced comparing with that in normal gravity.

Fig. 5 shows the scaling of CHF with the gravity, where $R' = d\sqrt{(\rho_l - \rho_v)g/4\sigma}$ is the dimensionless radius, and $q_{\text{Zuber}} = 0.131\rho_v^{1/2}h_{lv}(\sigma g(\rho_l - \rho_v))^{1/4}$ is the prediction of CHF by the Zuber correlation [5]. It is found that the Lienhard–Dhir model [6], established on the mechanism of hydrodynamic instability, gives a good prediction on the trend of CHF in different gravity conditions, although the value of R' is far beyond its initial application range. It is contrary to the traditional viewpoint on CHF's scale effect, which is based on the results in normal gravity.

In order to interpret this difference of the CHF scaling, a parameter L_{NS}, denoting the limit nucleate size, and a new dimensionless number $R'' = R/L_{\text{NS}}$ are introduced. CHF will occur due to the hydrodynamic

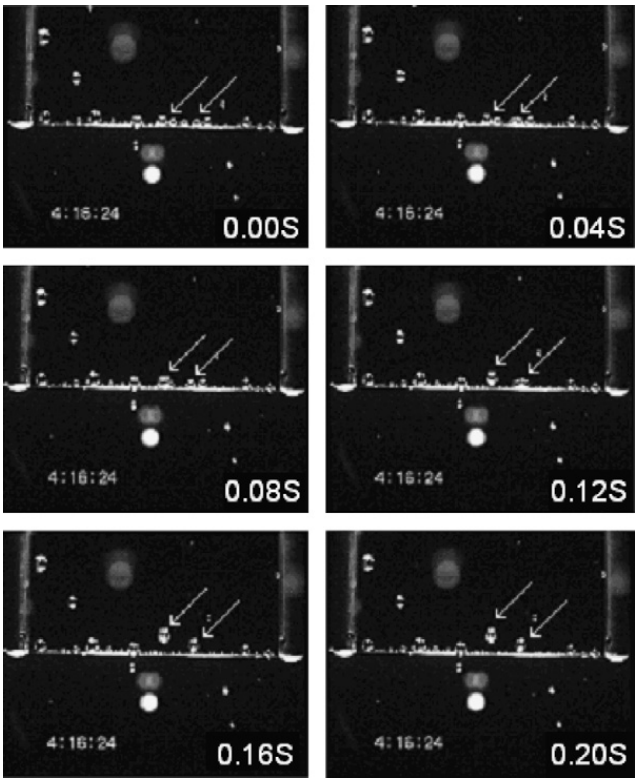

Fig. 6. Coalescence, vibration and departure of bubblers.

instability if R'' is larger, or if the heater diameter is much larger than the limit nucleation size. On the contrary, CHF will be caused by the mechanism of local dryout if R'' is smaller. It is believed that the parameter L_{NS} is independent with gravity. In the cases of the same heater used in different gravity, the value of R'' will keep constant whatever is the value of R', and the mechanism will then not alter. But on the ground, the value of R'' will decrease with the decrease of the heater radius, and the CHF mechanism will alter from the hydrodynamic instability to others. Thus, as mentioned above, a difference on the scaling of CHF will be observed. Further researches are needed for the delimitation of the two mechanisms.

3.2. Bubble dynamics and Marangoni effect

Fig. 6 shows the typical process of coalescence, vibration and departure of bubblers in the regime of fully developed nucleate pool boiling. It is found that the vibration due to coalescence of adjacent bubbles is the primary reason of bubble departure in microgravity in this regime. On the contrary, distinct bubble behaviors are observed in isolated bubble regime of nucleate pool boiling in microgravity (Fig. 7), comparing with those in normal gravity.

Author's personal copy

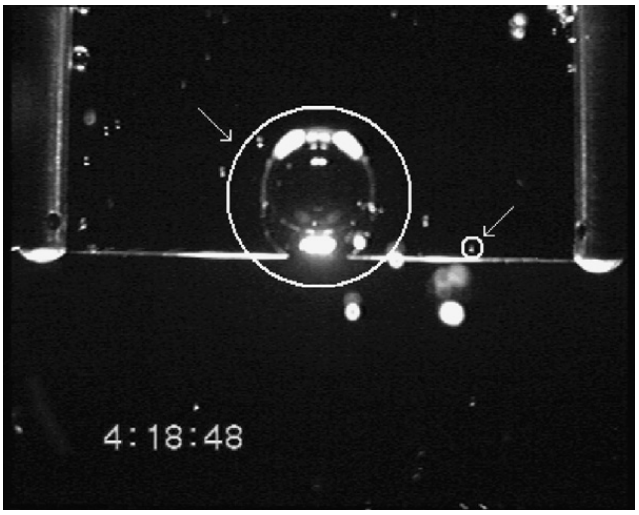

Fig. 7. Behaviors of isolated bubbles.

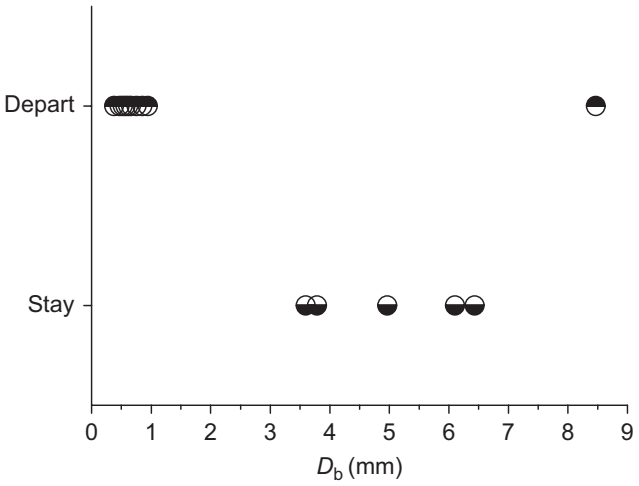

Fig. 8. Bubble departure diameters.

Fig. 8 plots the statistical data of isolated bubbles which appeared in the central section of the wire and departing along the direction parallel to the observing plane. It is found that three critical bubble diameters, namely $D_{b1} = 0.3$ mm, $D_{b2} = 3.5$ mm, $D_{b3} = 8.5$ mm, are observed in the space experiments, which divide the bubbles into four groups. The smallest bubbles with diameter less than 0.3 mm are continually forming and growing on the heater surface before departing slowly from the wire when their sizes exceed some critical value (0.3 mm). The bigger bubbles with diameter between 3.5 and 6.6 mm stay on the wire, oscillate along the wire, and coalesce with adjacent bubbles. The biggest bubble with diameter of the order of 10 mm, which is yielded during the onset of boiling, stays continuously on the wire and swallows continually up adjacent small bubbles till its diameter exceeds 8.5 mm at the CHF. The behaviors of small bubbles are observed both in microgravity and in normal gravity, while the last two kinds of bubble behaviors are observed only in microgravity aboard the satellite.

Presently, no model can predict the above observation. For example, the models of Karri [7] and Lee [8] predict, respectively, the departure diameter as 0.28 and 0.13 mm, close to the 1st bubble departure diameter, while the models of Fritz [9,10] and Zeng et al. [11] predict, respectively, the departure diameter as 10.9 and 7.1 mm, close to the 2nd bubble departure diameter observed in the present study. The reason may be that the Marangoni effect is ignored in these models. In microgravity environment, the interface effect will become a dominant factor because the buoyancy effect is extremely restrained and even eliminated. Commonly, the increase of temperature will lead the decrease of surface tension of liquid, thus the uneven temperature field will cause tangential forces that act on the interface, which pull the bulk fluid moving. This motion is usually called Marangoni convection. During the process of subcooled pool boiling, the temperature of the heater surface is higher than the saturation temperature, and the temperature of subcooled liquid far away from the heater surface is lower than the saturation temperature. Therefore, a distinct temperature gradient will be formed in the liquid around the bubble. Generally, the surface tension decreases as the increase of temperature. Then the Marangoni force will pull the bubble moving towards the high temperature side (namely the heater surface), which prevents the bubble from departing from the heater's surface. So the Marangoni force should be considered as the resistant force (F_R).

Let us consider the bubble Marangoni migration in the bulk liquid with a constant temperature gradient. If the wall effect and the variety of physical properties are ignored, the bubble Marangoni migration will finally reach a steady condition when the force due to Marangoni effect is balanced by the viscous drag force acting on the bubble. Therefore, the Marangoni force can be expressed as follows using the linear Stocks theory for the case of infinitesimal Reynolds and Marangoni numbers [12,13] as

$$F_m = 2K\pi|\sigma_T|T'R^2 \tag{1}$$

where σ_T, R and T' denote the temperature coefficient of surface tension, the bubble radius, and the temperature gradient, respectively. The empirical coefficient K is used to modify the departure from the linear theory for the case of finite Reynolds and Marangoni numbers.

Author's personal copy

Following Lee [8], other forces acting on the bubble can be expressed. Among them, the buoyancy force F_b, the inertia force F_i, and the pressure force F_p should be considered as the departure forces (F_D) since they pull the bubble to depart from the heater surface, while the drag force F_d and the surface tension force F_s should be considered as the resistant forces (F_R) since they prevent the bubble from departing from the heater's surface. Therefore, the sum of the forces acting on the bubble is,

$$F = F_D - F_R = (F_i + F_p + F_b) - (F_d + F_s + F_m) \tag{2}$$

Following Karri [7] and Lee [8], an asymptotic bubble growth relation can be assumed

$$R = E\tau^{1/2} \tag{3}$$

where τdenotes the time after the bubble forming, while the empirical parameter E is calculated by the relation given by Cole and Shulman [14]

$$E = \frac{1}{2\sqrt{\pi}} Ja\sqrt{\alpha_l} \tag{4}$$

where, Ja and α_l are the Jacob number and the heat diffusivity coefficient of liquid.

In this way, formula (2) can be rewritten as

$$f(y) = C_4 y^4 + C_3 y^3 + C_1 y + C_0 \tag{5}$$

where,

$$y = \tau^{1/2} \tag{6}$$

$$C_4 = \tfrac{4}{3}\pi E^3(\rho_L - \rho_V)g \tag{7}$$

$$C_3 = -2K\pi|\sigma_T|T'E^2 \tag{8}$$

$$C_1 = 4\sigma R_0 \sin^2\beta + \frac{\pi}{3}\rho_L E^4 \tag{9}$$

$$C_0 = R_0 E^3 \rho_L \sin^2\beta\left(\tfrac{1}{3} - \tfrac{3}{8}C_d\right) \tag{10}$$

in which β and C_d denote the contact angle and drag coefficient, respectively.

According to Eqs. (2) and (5), the following conclusion can be obtained: if $f(y) < 0$, the departure force is larger than the resistant force, so the bubble will stay on the heater's surface; if $f(y) > 0$, the departure force is smaller than the resistant force, so the bubble will depart from the heater's surface.

Using the following parameters for R113 are used, $p_l = 0.1$ MPa, $\Delta T_{sub} = 26\,^\circ$C, $\Delta T_{sat} = 30\,^\circ$C, $\beta = 5^\circ$, $K = 0.035$, the varieties of $f(y)$ with gravity are plotted in Fig. 9, where the abscissa is replaced by the bubble diameter with Eq. (3).

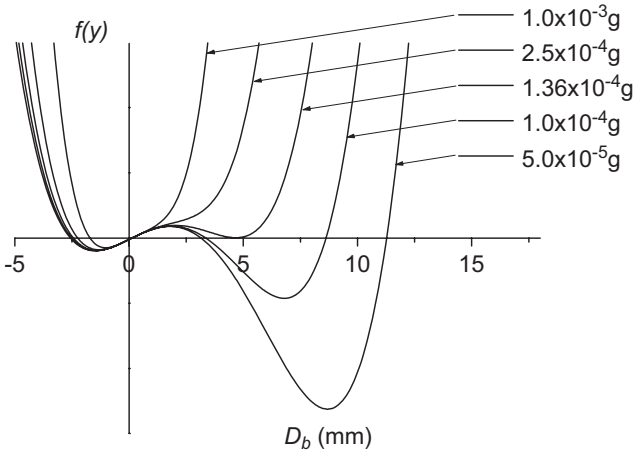

Fig. 9. Variety of $f(y)$ with gravity.

Considering the positive half plane of D_b, there is only one point of intersection between Eq. (5) and the abscissa, i.e. $D_{b1} \approx 0.11$ mm, in normal gravity. It is very close to that predicted by Lee's model, which shows that the effect of Marangoni convection can be ignored in normal gravity. This value is gradually increasing as the residual gravity decreasing, although the increment is very tiny. On the contrary, when the gravity reduces to $1.36 \times 10^{-4}g$, a second point D_{b2} of intersection between Eq. (5) and the abscissa appears. Furthermore, when the gravity is less than $1.36 \times 10^{-4}g$, there are three points of intersection (D_{b1}, D_{b2}, and D_{b3}) between Eq. (5) and the positive abscissa, which divide the positive abscissa into four regions:

(1) $D_b < D_{b1}$, $f(y) < 0$, the bubble stays on the heater surface;
(2) $D_{b2} > D_b > D_{b1}$, $f(y) > 0$, the bubble departs from the heater surface;
(3) $D_{b3} > D_b > D_{b2}$, $f(y) < 0$, the bubble stays on the heater surface; and
(4) $D_b > D_{b3}$, $f(y) > 0$, the bubble departs from the heater surface.

It agrees qualitatively with the observation in space experiment. Furthermore, a quantitative agreement can also be obtained with $K = 0.035$, in which $D_{b1} = 0.11$ mm, $D_{b2} = 3.4$ mm, $D_{b3} = 8.6$ mm are predicted.

4. Conclusion

A temperature-controlled pool boiling (TCPB) device has been developed to study the bubble behavior and heat transfer in subcooled pool boiling phenomenon both in normal gravity and in microgravity. The space

Author's personal copy

experiment has been performed aboard the 22nd Chinese recoverable satellite, while the ground experiments have also been conducted before and after the flight.

Three modes of heat transfer, namely single-phase natural convection, nucleate boiling, and two-mode transition boiling, are observed. The analysis of single phase convection verifies the reliability of experimental facility and confirms the residual gravity level on the satellite as 10^{-3}–$10^{-5}g$. It is found that the temperature of the onset of boiling is independent of the gravity level. It is also found that the heat transfer of nucleate pool boiling is slightly enhanced in microgravity comparing with those in normal gravity. It is also found that the correlation of Lienhard and Dhir [6] can predict the CHF with good agreement, although the range of the dimensionless radius is extended by three or more decades above the originally set limit.

On the contrary, distinct bubble behaviors are observed in isolated bubble regime of nucleate pool boiling in microgravity, comparing with those in normal gravity. Three critical bubble diameters are observed in microgravity, which divide the observed vapor bubbles into four regimes with different sizes. Considering the Marangoni effect, a qualitative model is proposed to reveal the mechanism underlying the bubble departure processes, and a quantitative agreement can also be acquired.

Acknowledgments

The present study is supported financially by the Chinese Academy of Sciences under the Grant of KJCX2-SW-L05, and the National Natural Science Foundation of China under the Grant of 10432060. The authors also wish to acknowledge the fruitful discussion with Prof. H. Ohta (Kyushu University, Japan).

References

[1] J. Straub, Boiling heat transfer and bubble dynamics in microgravity, Advances in Heat Transfer 35 (2001) 57–172.
[2] P. Di Marco, W. Grassi, Motivation and results of a long-term research on pool boiling heat transfer in low gravity, International Journal of Thermal Science 41 (2002) 567–585.
[3] S.X. Wan, J.F. Zhao, G. Liu, W.R. Hu, TCPB device: description and preliminary ground experimental results, in: 54th International Astronautical Congress, September 29–October 3, 2003, Bremen, Germany.
[4] T.H. Kuehn, R.J. Goldstein, Correlating equations for natural convection heat transfer between horizontal circular cylinders, International Journal of Heat Mass Transfer 19 (1976) 1127–1134.
[5] N. Zuber, Hydrodynamic aspects of boiling heat transfer, Ph. D. Thesis, UCLA, Los Angeles, CA, USA, 1959.
[6] J.H. Lienhard, V.K. Dhir, Hydrodynamic prediction of peak pool boiling heat fluxes from finite bodies, Journal of Heat Transfer—Transactions of the ASME 95 (1973) 152–158.
[7] S.B.R. Karri, Dynamics of bubble departure in micro-gravity, Chemical Engineering Communications 70 (1988) 127–135.
[8] D.J. Lee, Bubble departure radius under microgravity, Chemical Engineering Communication 117 (1992) 175–189.
[9] W. Fritz, W. Ende, Berechnung des maximalvolumens von dampfslasen, Physik 36 (1935) 379–384.
[10] W. Fritz, W. Ende, Uber den verdampfungsvorgang nach kinematographischen aufnahmen an dampfblasen, Physik 37 (1936) 391–401.
[11] L.Z. Zeng, J.F. Klausner, R. Mei, A unified model for the prediction of bubble detachment diameters in boiling system—1. Pool boiling, International Journal of Heat Mass Transfer 36 (1993) 2261–2270.
[12] K.G. Batchelor, An Introduction to Fluid Dynamics, Cambridge University Press, Cambridge, 1994.
[13] N.O. Young, J.S. Goldstein, M.J. Block, The motion of bubbles in a vertical temperature gradient, Journal of Fluid Mechanics 6 (1959) 350–356.
[14] R. Cole, H.L. Shulman, Bubble growth rates at high Jakob numbers, International Journal of Heat Mass Transfer 9 (1966) 1377–1390.